

# Study of a New Kind of Multipulse Rocket Motor

Mingde Song\*

*Northwestern Polytechnic University, 710072 Xi'an, People's Republic of China*

and

Dingyou Ye†

*Shaanxi Power Machinery Institute, 710025 Xi'an, People's Republic of China*

A new method for multi-ignitable rocket motor design has been proposed in this paper, by analyzing flow, heat-transfer, and combustion of a non-Newtonian pasty propellant, in which oxidizer and fuel binder are mixed homogeneously. The new motor has advantages found in both solid- and liquid-propellant rocket motors. The motor discussed in this paper is also thrust adjustable. Moreover, because the propellant is ignited by surplus heat from the combustion chamber no additional ignition energy is needed. The key technology of this new method is the proposed reignitable igniter. A two-dimensional flow and heat-transfer model of the propellant inside the reignitable igniter has been developed. Control equations have also been solved numerically. Propellant temperatures inside the igniter holes have been obtained, in conjunction with a simple ignition criterion. The relationship between igniter temperatures, igniter length, igniter diameter, and drive pressure has also obtained. A combustion model applicable to the new pasty propellant is proposed on the basis of the current solid-propellant BDP (Beckstead-Derr-Price) combustion model. A prototype test apparatus has also been built for multipulse firing. Seven operation pulses were obtained. Each pulse lasts about 5 s, and the time interval between pulses is approximately 2 s.

## Nomenclature

$A$	=	area
$k$	=	consistency coefficient
$L$	=	length
$m$	=	mass
$n$	=	flow exponent
$P$	=	pressure
$\dot{Q}$	=	flow mass rate
$R$	=	radius
$r$	=	burning rate
$T$	=	temperature
$t$	=	time
$u$	=	velocity
$x, y$	=	coordinate
$\eta$	=	viscous coefficient
$\lambda$	=	heat conduct coefficient
$\mu$	=	dynamic viscous coefficient
$\rho$	=	density
$\tau$	=	shear stress

## Introduction

A MULTIPULSE restartable rocket motor has many advantages in aerospace propulsion. It is beneficial to the improvement of missile performance and guidance features. A liquid-propellant rocket motor is restartable, but the leak of liquid propellant is hazardous. It is also a relatively complicated system. A solid rocket motor is simple, but it is difficult to restart. Many approaches have been proposed to solve this problem, such as the compartment pulse rocket motor,<sup>1</sup> water-extinguished pulse rocket motor,<sup>2</sup> hybrid rocket motor,<sup>3</sup> gelled-propellant rocket motor,<sup>4</sup> and pasty-propellant rocket motor.<sup>5</sup>

In this paper we propose a new design method for multi-ignitable pulse rocket motors by analyzing flow and heat transfer of a pasty

propellant. In our research pasty propellant is a non-Newtonian propellant consisting of oxidant powder and polymer fuel filler mixed homogeneously, like unsolidified solid propellant. The proposed reignitable igniter is a metal cylinder with a number of high-length/diameter ( $L/D$ ) ratio circular holes with particular temperature distribution. The pasty propellant is heated and ignited or cooled and extinguished when flowing through the high- $L/D$  circular holes. The reignition energy comes from the rocket combustion chamber; therefore, no additional ignition energy is needed.

Theoretically, the pulse number of the new rocket motor is unlimited, and the thrust could be adjusted by controlling pasty propellant flow rate.

## Introduction of the New Motor

The new multipulse rocket motor is composed of drive device, pasty propellant and tank, flow control system, first-pulse igniter, reignitable igniter, combustion chamber, nozzle and pressure feedback system, as shown in Fig. 1.

The reignitable igniter is a metal cylinder with a number of high- $L/D$  circular holes. The temperature distribution in the igniter is quite important. The length to the left of point  $P$  is outside the combustion chamber and is at a low temperature. The length to the right of point  $P$  is inside the combustion chamber and is at the temperature of the combustion chamber. The combustion chamber possesses a high temperature after the motor's first operation, which is ignited by a normal pyrogen-type igniter. Figure 2 shows a reignitable igniter with one hole.

The non-Newtonian pasty propellant flows into the combustion chamber through the igniter when the drive pressure is on and is ignited by the first pulse igniter (pyrogen-type igniter). When we want the motor to stop operating, we remove the drive pressure, and the propellant no longer flows into the combustion chamber. Obviously, propellant temperature in the igniter left end decreases as a result of the heat loss in the low temperature field. The heat loss makes the burning propellant extinguish if the left end temperature is low enough and the heat loss is large enough. When we exert the drive pressure again, the propellant will again flow into the combustion chamber and is heated during its flow through the holes in the high-temperature right end of the igniter. The propellant will be ignited if its mean temperature reaches a critical level at some points to the right of  $P$ . The motor will then begin to operate once more. By controlling propellant flow rate, the thrust is also adjustable.

Presented as Paper 98-3849 at the AIAA/ASME/SAE/ASEE 34th Joint Propulsion Conference and Exhibit, Cleveland, OH, 13–15 July 1998; received 1 March 1999; revision received 15 August 2000; accepted for publication 25 September 2000. Copyright © 2000 by the American Institute of Aeronautics and Astronautics, Inc. All rights reserved.

\*Senior Engineer; currently Research Associate, Department of Mechanical and Aerospace Engineering, University of Southern California, Los Angeles, California, 90089; mdsong@263.net. Member AIAA.

†Professor and President, Department of Aerospace Engineering.

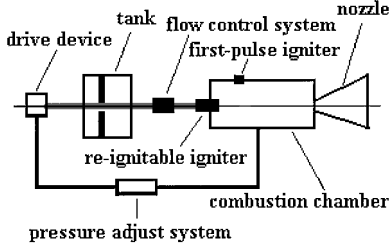


Fig. 1 Sketch of the new multipulse pasty propellant rocket motor.

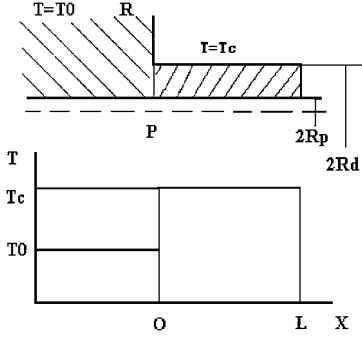


Fig. 2 Reignitable igniter with one high-L/D hole.

A pressure-feedback system adjusts the drive pressure coupled with the combustion chamber pressure.

The propulsive force from this motor is determined by propellant flow mass rate, not by burning surface area. Like solid rocket motors the pasty propellant is also of a higher density and avoids hazardous leaks.

It is necessary to study the critical  $L/D$  ratio of the circular holes in both the left and the right portions of the igniter to ensure a reliable extinguishment or ignition. For example, if the ignition length at a certain radius is not long enough the propellant will not be ignited. If the length is too long, the extra length increases the inert weight.

### Theoretical Analysis

We assume the following:

- 1) Pasty propellant obeys a laminar power law for fluids with constant physical properties.
- 2) Velocity and temperature profiles of the propellant are fully developed.
- 3) Pressure gradient on the propellant is constant.
- 4) Effects of axial heat transfer, inlet effect, and capillary action can be neglected.
- 5) Combustion chamber temperature distribution is uniform.
- 6) Propellant will be ignited at a critical temperature level.

Velocity and volume flow rate of pasty propellant through igniter hole can be expressed as

$$u = [n/(n+1)](\Delta P/2kL)^{1/n}(R^{(n+1)/n} - r^{(n+1)/n}) \quad (1)$$

$$Q = \pi(\Delta P/2kL)^{1/n}[n/(1+3n)]R^{(1+3n)/n} \quad (2)$$

According to Eqs. (1) and (2), flow rate of non-Newtonian fluid ( $n < 1$ ) is more sensitive than that of Newtonian fluid ( $n = 1$ ). Flow rate of Newtonian fluid increases to  $2Q$  from  $Q$  when drive pressure increases to  $2P$  from  $P$ , whereas that of non-Newtonian fluid ( $n = 0.5$ ) increases to  $4Q$ . Therefore, propellant flow rate and motor thrust can be controlled by adjusting drive pressure. This is one of the advantages of pasty propellant rocket motor.

During the ignition process, heat transfer between the igniter and combustion chamber and between the igniter and propellant occur only to the right of point  $P$ , as shown in Fig. 2, so, we only need to analyze heat transfer to the right of point  $P$ .

Control equations for the pasty propellant in the igniter are as follows:

Momentum equation:

$$\rho_p \frac{\partial u_p}{\partial t} + \frac{\partial P}{\partial x} = \frac{1}{r} \frac{\partial}{\partial r} \left[ r \eta_0 \left( \frac{\partial u_p}{\partial r} \right)^n \right] \quad (3)$$

Energy equation:

$$\rho_p c_p \left( \frac{\partial T_p}{\partial t} + u \frac{\partial T_p}{\partial x} \right) = \frac{\lambda_p}{r} \frac{\partial}{\partial r} \left( r \frac{\partial T_p}{\partial r} \right) + \lambda_p \frac{\partial^2 T_p}{\partial x^2} + \eta_0 \left( \frac{\partial u_p}{\partial r} \right)^{n+1} + Q_w + Q_x \quad (4)$$

According to assumption (4),

$$Q_x = 0$$

Before propellant ignition

$$Q_w = 0$$

after propellant ignition

$$Q_w = \rho_p q_p Z e^{-E_p/RT}$$

Heat-transfer equation of reignitable igniter is

$$\rho_d c_d \frac{\partial T_d}{\partial t} = \frac{\lambda_d}{r} \frac{\partial}{\partial r} \left( r \frac{\partial T_d}{\partial r} \right) + \lambda_d \frac{\partial^2 T_d}{\partial x^2} \quad (5)$$

Velocity distribution in the pasty propellant can be rewritten as

$$u = [n/(n+1)](\Delta P/2kL)^{1/n} R^{(n+1)/n} [1 - (r/R)^{(n+1)/n}]$$

Propellant mean temperature is

$$T_{av} = \frac{\int_0^R P 2\pi r dr u_p c_p T_p}{\int_0^R P 2\pi r dr u_p c_p} \quad (6)$$

Boundary conditions for the pasty propellant are

$$r = 0, \quad \frac{\partial T}{\partial r} = 0 \quad (7)$$

$$x = 0, \quad T = T_0 \quad (8)$$

$$x = L, \quad T = T_c \quad (9)$$

Boundary conditions for the igniter are

$$x = 0, \quad T = T_0 \quad (10)$$

$$r = R_d, \quad \lambda_d \frac{\partial T_d}{\partial x} = q_d \quad (11a)$$

or

$$r = R_d, \quad T_d = T_c \quad (11b)$$

At the interface between the propellant and igniter, the coupling relation is

$$r = R_p, \quad \lambda_p \frac{\partial T_p}{\partial r} = \lambda_d \frac{\partial T_d}{\partial r} \quad (12)$$

According to assumption (6), if propellant temperature at  $x = x_{ig}$  increases to a critical level  $T_{ig}$  it will be ignited, that is to say, the ignition criterion is

$$T_{av}(x_{ig}) \geq T_{ig} \quad (13)$$

The boundary condition

$$x = L, \quad T = T_c \quad (14)$$

should be changed to

$$x \geq x_{ig}, \quad T = T_c \quad (15)$$

after propellant ignition.

Extinguishment is needed to prevent propellant combustion from continuing back into the propellant tank causing detonation. When the drive pressure is removed, the propellant stops flowing. However, combustion will no doubt continue to the right of  $P$  because the temperature in this end is still at the combustion chamber temperature. Therefore we only need to analyze propellant combustion to the left of  $P$  when studying extinguishment.

Propellant combustion heat dissipates when combustion withdraws back to the left of  $P$  because the temperature of the igniter hole surface decreased sharply to a very lower temperature  $T_L$ . If the propellant reaction heat cannot maintain propellant burning as a result of the large heat loss, combustion will cease. We should say that, to satisfy this requirement, the igniter hole radius should not be too large. This requirement can also be satisfied by keeping the left end temperature very low.

The analysis of extinguishment is similar to that of the ignition process, but the effects of the source item should be taken into account. In this paper we introduce a very simple extinguishment criterion:

$$T_{av}(x_{ig}) \leq T_{ex} \quad (16)$$

### Results and Discussion

Control equations for the propellant and reignitable igniter have been solved numerically. The igniter temperature and the propellant temperature are coupled in the interface. The input parameters for the calculation are listed here:  $L_R = 0.060$  m;  $L = 0.130$  m;  $R_d = 0.01$  m;  $T_i = 300$  K;  $R_p = 0.001$  m;  $\rho_p = 1700$  kg/m<sup>3</sup>;  $c_p = 1380$  J/kgK;  $\lambda_p = 0.6813$  J/mK;  $\rho_d = 19,000$  kg/m<sup>3</sup>;  $\Delta P = 0.5$  MPa;  $c_d = 132$  J/kgK;  $\lambda_d = 727.32$  J/mK;  $n = 0.896$ ;  $k = 212.41$ ;  $\eta = 100$  Pa s,  $T_c = 1500$  K; and  $\rho_p = 1700$  kg/m<sup>3</sup>.

Relationships between combustion chamber temperature and igniter length, igniter inner diameter, propellant extinguishment temperature and propellant combustion heat generation for steady operation have been calculated and are shown in Figs. 3–6. In these

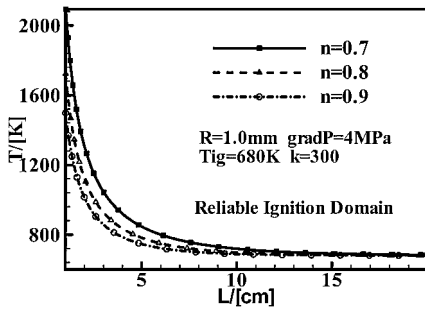


Fig. 3 Critical lengths of the reignitable igniter at different chamber temperature.

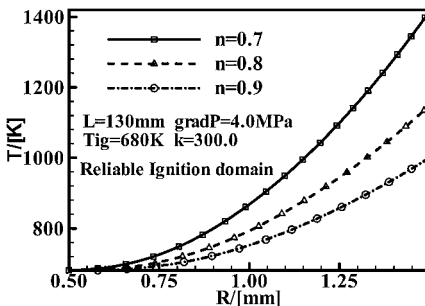


Fig. 4 Critical radius of the reignitable igniter holes at different chamber temperature.

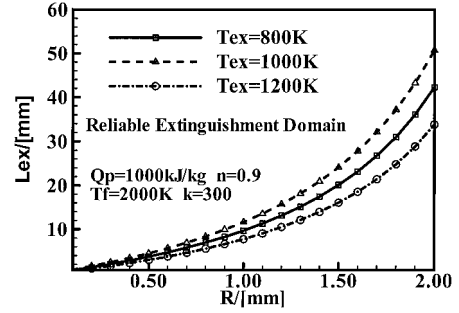


Fig. 5 Critical length and diameter of the igniter holes to ensure a reliable extinguishment at different propellant extinguishment temperature.

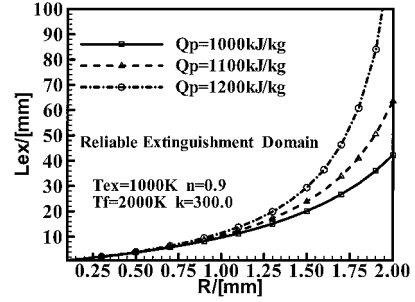


Fig. 6 Critical length and diameter of the igniter holes to ensure a reliable extinguishment at different combustion heat generation of propellants.

figures every point on the curve represents the critical condition points for steady operations.

Figure 3 indicates that ignition reliability at low chamber temperature can be increased by increasing igniter length in the chamber. This also means that the time interval between pulses can be increased by increasing igniter length. The area above the curve is the ignition domain; propellant will be ignited successfully in this area. The area below the curve is the non-ignition domain.

There is an optimum range for igniter length (Fig. 3). If the igniter length is too short, the chamber temperature should be much higher to ensure propellant ignition; if the length is too long, although the propellant can be ignited at a relatively low temperature, the length may be too long to be efficient. This range can be obtained by analyzing the variation of the derivative of the function  $T_R = f(L_2)$ .

The time interval between pulses depends also on the  $L/D$  ratio. Because the chamber temperature drops after a pulse as time goes on, if some measure is taken to keep the right end at a constant temperature this difficulty can be overcome.

Figure 4 shows that for a larger hole radius a higher chamber temperature is needed.

Figure 5 shows the relationship between propellant extinguishment temperature and igniter extinguishment distance. The higher the propellant extinguishment temperature, the shorter the igniter extinguishment distance should be.

Figure 6 shows the effect of propellant combustion heat generation on extinguishment distance. The higher the propellant combustion heat generation is, the longer the igniter extinguishment distance should be. Calculated results also indicate that there is not a practical extinguishment distance if the propellant combustion heat generation is too high. For example, if propellant heat generation exceeds 1500 kJ/kg, for an 8-mm diam igniter hole we cannot obtain an extinguish distance in the calculation.

Relationships between drive pressure, propellant ignition temperature, propellant flow characteristics,  $n$ ,  $k$  and chamber temperature can be also obtained with the preceding method.

Propellant flow velocity is theoretically equal to propellant burning rate to ensure a steady operation. Because propellant burning rate is dependent on motor chamber pressure, the relationship between

propellant flow rate and burning rate is quite complex. That is partly the reason why a pressure feedback system should be introduced.

We would like to point out that the extinguishment distance might be longer than the calculated one because the constant temperature boundary condition is not practical in real motors. Moreover, propellant does not extinguish immediately when the proposed extinguishment criterion is satisfied.

### Propellant Combustion Behavior

As mentioned, flow velocity and burning rate should be equal to ensure a steady operation. A study of the burning rate of pasty propellant is essential. The pasty propellant we used in this research is similar to an unsolidified solid composite propellant slurry in chemical and physical characteristics. Therefore, we study the pasty propellant combustion behavior on the basis of present solid propellant BDP models.<sup>6</sup> A new parameter named pasty propellant energy effect is introduced to express energy difference between the two kinds of propellant. If this new parameter is neglected, this model becomes the solid propellant BDP model.

Mass burning rate of pasty propellant and its gradients during steady combustion process can be expressed as

$$m_r = (m_{ox}/\alpha)(s_{ox}/s_0) = [m_f/(1 - \alpha - \varepsilon)](s_f/s_0) \quad (17)$$

$$m_{ox} = \rho_{ox} r_{ox} = Z_{ox} e^{-E_{ox}/RT_s} \quad (18a)$$

$$m_f = \rho_f r_f = Z_f e^{-E_f/RT_s} \quad (18b)$$

The energy equation considering pasty propellant energy effect  $Q_{sur}$  and aluminum powder heat effect can be written as

$$\begin{aligned} c_p m (T_s - T_0) + \alpha m Q_{ox} + (1 - \varepsilon - \alpha) m Q_f + \varepsilon m Q_{Al} + m Q_{sur} \\ = \beta_F m Q_{PF} e^{-\xi_{PF}} + (1 - \beta_F) \alpha m [(1 - \eta) Q_{AP} e^{-\xi_{AP}} \\ + Q_{FF} e^{-\xi_{FF}}] + \alpha \eta m Q_{AP} \end{aligned} \quad (19)$$

Flame diffusion distance  $x_d$  can be obtained from BDP model as

$$\bar{x}_d = A_{th} x_d \quad (20)$$

Oxidizer particle diameter should be the equivalent diameter if particle diameter distribution is considered:

$$D_{ef} = \sum_{i=1}^n \text{sig}(i) e^{\theta(i)}, \quad \theta(i) = \frac{1}{2} [\ln D_{max} + \ln D_{min}] \quad (21)$$

Details of other expressions can be obtained easily from the BDP combustion model in Ref. 6. The input parameters used in the calculations are listed here:  $Z_{ox} = 3 \times 10^6$  m/mols;  $E_{ox} = 9.2 \times 10^4$  J/mol;  $Z_f = 2.5 \times 10^3$  m/mols;  $E_f = 6.27 \times 10^4$  J/mol;  $\rho_{AP} = 1950$  kg/m<sup>3</sup>;  $\rho_f = 1270$  kg/m<sup>3</sup>;  $\rho_{Al} = 2700$  kg/m<sup>3</sup>;  $\delta_{AP} = 1.8$ ;  $\delta_{PF} = 1.5$ ;  $A_{th} = 0.3$ ;  $Q_{sur} = 30,000$  J/mol;  $Q_{ox} = 501,600$  J/mol;  $Q_{Al} = -204,400$  J/mol; and  $Q_f = -209,000$  J/mol.

The effect of pasty propellant energy effect is shown in Fig. 7. There is a higher burning rate and a higher pressure exponent when a propellant has a higher pasty propellant energy effect. That is to

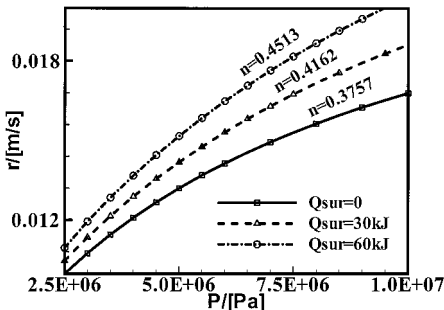


Fig. 7 Calculated burning rate at different pasty propellant energy effects.

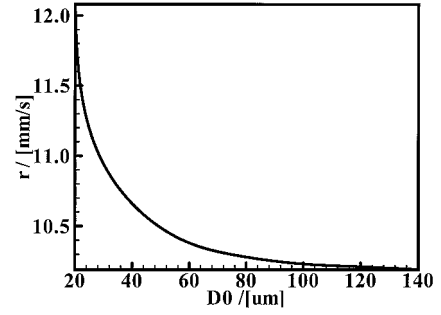


Fig. 8 Calculated burning rate of propellants with different oxidizer particle sizes.

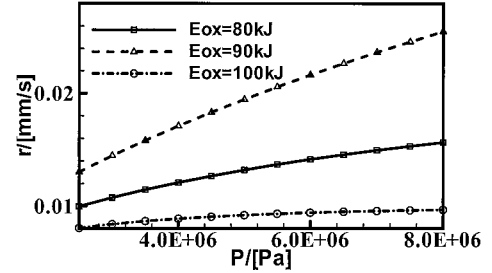


Fig. 9 Calculated burning rate at different oxidizer activation energy.

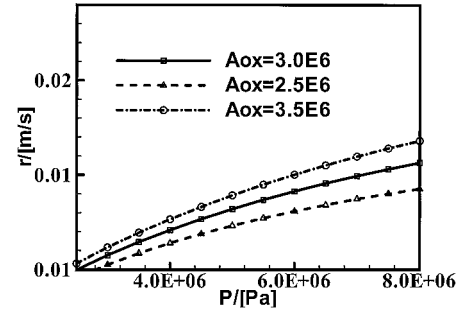


Fig. 10 Calculated burning rate at different oxidizer exponent coefficient.

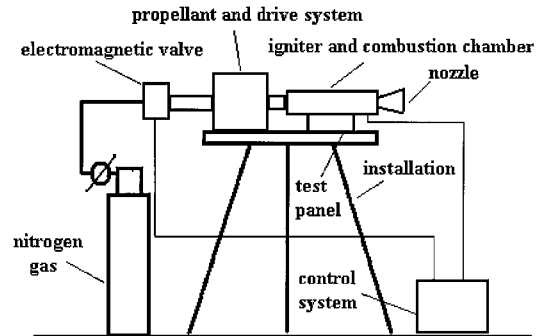


Fig. 11 Sketch of the experiment system of the prototype motor.

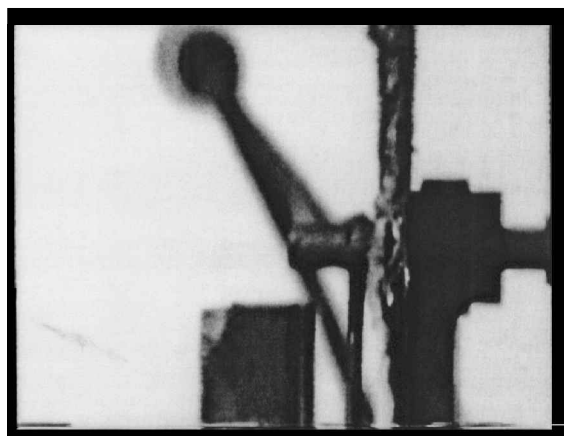
say, the pasty propellant and propellant slurry has a higher burning rate than its solidification. This has been proved by experimentally.<sup>7</sup>

Figure 8 shows the effect of oxidizer particle diameter on pasty propellant burning rate. A propellant with a fine particle diameter possesses a higher burning rate.

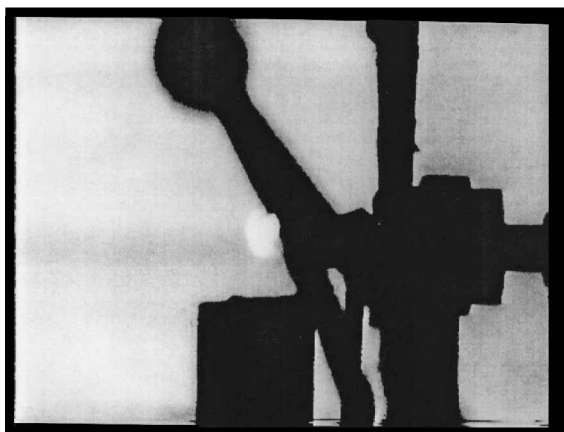
Effects of the catalyst on burning rate are shown in Figs. 9 and 10. Increasing the exponent coefficient and decreasing the activation energy both lead to an increase in pasty propellant burning rate.

### Experiment Results

An experimental installation has been built to study the operational behavior of the pulse rocket motor designed using the method just described. The installation is shown in Fig. 11.



a) Extinguishment



b) Reignition



c) Steady combustion

**Fig. 12** Images of flame in the igniter right end holes taken by Kodak Ektapro High Speed Motion Analyzer.

The main purpose of the experiment in this preliminary stage is to investigate the operational behavior of the reignitable igniter, especially its ignition and extinguishment abilities, and also the ignition and combustion process of the pasty propellant in the new motor. These phenomena are observed in a test motor with glass windows.

A Kodak Ektapro High Speed Motion Analyzer, which takes 1000 images per second, and a Sony video recorder have also been used

to investigate the ignition and combustion processes of the pasty propellant.

Because the pressure and propulsive forces on the motor are not of primary interest in this stage of the research, there are only three laser-machined circular holes in the igniter. The length of each hole is 130 mm, and the radius of each hole is 1.0 mm. The reignitable igniter is made of a high-temperature tungsten-copper alloy. The temperature of the igniter right end is maintained at 1073 K and that of the left end at 300 K. The pasty propellant used in the experiment is very similar to an unsolidified composite propellant slurry. Details of the pasty propellant can be found in Ref. 8.

Seven pulses have been obtained by controlling propellant flow rate with an electromagnetic valve. Each pulse lasts approximately 5 s, with the time interval between two pulses of approximately 2 s.

The images taken by the motion analyzer show that the ignition and combustion process of the pasty propellant are basically steady during the operations. Figure 12 shows the typical images of the flame in reignition and operation periods.

The main problem we had in the experiment was that the extinguishment response time of the motor was rather long. One of the reasons was that the propellant, which remains in the holes, still burns. Also the propellant still flows for some time as a result of the inertia force after drive pressure cutoff.

## Conclusions

A new restartable pulse pasty propellant rocket motor design method has been presented. Preliminary theoretical and experimental results are presented in this paper. The main technology of the method is the designing of the reignitable igniter. Igniter length, inner radius, combustion chamber temperature, time interval between two pulses, drive pressure, and propellant characteristics determine the operation behavior of the motor.

Future work will be focused on experiments with larger propulsive force motor. Studies will be done to value the relationship between time interval and propellant combustion temperature and how to accelerate the response time during the start and extinguishment process.

## Acknowledgments

This work is supported by China National Science Foundation (NSFC). The financial support from NSFC is highly appreciated. We also wish to express our thanks to D. Jia for his help in the numerical calculation and S. Chen, from HongXing Chemical Institute, for providing the pasty propellant samples.

## References

- <sup>1</sup>Nishii, S., Fukuda, K., and Kubota, N., "Combustion Tests of Two-Stage Rocket Motors," AIAA Paper 89-2426, July 1989.
- <sup>2</sup>Strand, L. D., and Gerber, W., "A Study of SPRM Command Termination by Water Injection," AIAA Paper 70-641, June 1970.
- <sup>3</sup>Grenda, J., and Merkle, C., "Numerical Simulation of Combustion Instability in Hybrid Rocket Motors," AIAA Paper 94-2879, June 1994.
- <sup>4</sup>Yasuhara, W. H., "Advanced Gel Propulsion Controls for Kill Vehicles," AIAA Paper 93-2636, June 1993.
- <sup>5</sup>Kukushkin, V., "The Pasty Propellant Rocket Engine Development," AIAA Paper 93-1754, June 1993.
- <sup>6</sup>Beckstead, M. W., Derr, R. L., and Price, C. F., "A Model of Composite Solid Propellant Combustion Based on Multiple Flames," *AIAA Journal*, Vol. 8, No. 12, 1970, pp. 2200-2207.
- <sup>7</sup>Song, M., Wu, X., and Ye, D., "Flow, Heat Transfer and Ignition Analysis of Premixed Flammable Fluid in Large  $L/D$  Tubes," *Journal of Propulsion Technology*, Vol. 18, No. 3, 1997, pp. 51-55.
- <sup>8</sup>Song, M., and Ye, D., "Numerical Simulation and Experimental Study of Pasty Propellant and Solid Propellant Slurry Steady Combustion Behavior," *Journal of Solid Rocket Technology*, Vol. 21, No. 4, 1998, pp. 8-12.